School of Life and Pharmaceutical Sciences[1], Dalian University of Technology, Panjin; The Second Hospital of Dalian Medical University[2], Dalian, China

Anti-CD19 mAb-conjugated human serum albumin nanoparticles effectively deliver doxorubicin to B-lymphoblastic leukemia cells

H. Pan[1], S. Li[1], M. Li[1], Q. Tao[1], J. Jia[1], W. Li[2], L. Wang[1], Z. Guo[1], K. Ma[1], Y. Liu[1,*], C. Cui[1,*]

Received March 6, 2020, accepted April 17, 2020

**Corresponding authors: Changhao Cui, Yajun Liu, School of Life and Pharmaceutical Sciences, Dalian University of Technology, Panjin 124221, China*
changhaocui@dlut.edu.cn, yjliu85@dlut.edu.cn

Pharmazie 75: 318-323 (2020) *doi: 10.1691/ph.2020.0026*

B-Lymphoblastic leukemia (B-LL) is the most common childhood hematological malignancy. Although its overall prognosis is good, the outcome after relapse is poor. CD19 is highly expressed on the membrane of most malignant B-cells, and was shown to be a promising therapeutic target of B-LL. In this present work, we designed and synthesized a novel drug carrier, anti-CD19 monoclonal antibody-conjugated human serum albumin nanoparticles (HSA-CD19 NPs). Doxorubicin (DOX) was well encapsulated into the HSA-CD19 NPs to form an anticancer nanodrug DOX/HSA-CD19. DOX/HSA-CD19 was preferentially uptaken by $CD19^+$ B-LL cell line KOPN-8. DOX/HSA-CD19 showed strong antiproliferative effect on KOPN-8 cells with an IC_{50} value of 4.1 μg/mL. Further, proapoptotic Bax and caspase-3 were significantly elevated, but antiapoptotic Bcl2 was reduced in DOX/HSA-CD19 treated KOPN-8 cells, indicating the activation of the apoptosis pathway by the nanodrug. By contrast, DOX/HSA-CD19 did not show affinity to CD19-monocytic cell line, U937, and did not affect its proliferation. Collectively, HSA-CD19 NPs are a kind of effective novel drug carrier, and DOX/HSA-CD19 is a promising antitumor nanodrug for the treatment of B-LL.

1. Introduction

Leukemia, a hematopoietic malignancy, accounts for 2.4% of all cancer cases and 3.2% of all cancer deaths in 2018 (Bray et al. 2018). B-Lymphoblastic leukemia (B-LL) is a major type of childhood and adolescent leukemia characterized by abnormal proliferation of primitive and immature B cells in the bone marrow (Akiyama et al. 2008). Current therapeutic strategies for B-LL include chemotherapy, hematopoietic stem cell transplantation and chimeric antigen receptor T-cell immunotherapy (CAR-T) (Giavridis et al. 2018; Yang et al. 2019). However, these strategies displayed clear limitations. For example, drug resistance is common in chemotherapy (Wei et al. 2017), and bone marrow transplantation is often hampered by limited donors. CAR-T treatment is effective in the treatment of B-LL but frequently involved in safety concerns because serious adverse effects such as cytokine release syndrome and neurotoxicity can occur (Ghorashian et al. 2019; Schuster et al. 2019) . Therefore, there is still an urgent need for the development of new therapeutic strategies for more effective and specific treatment of B-LL.

Therapeutic approaches for B-LL with CD19 as a target have recently been reported. CD19 is a member of the immunoglobulin super-family, which is exclusively expressed on the surface of B lymphocytes (Wang et al. 2012). CD19 is a critical co-receptor of B cell antigen receptor, providing an effective binding site for respective immunoconjugates for diagnosis and treatment of B-cell malignancies. Nanoparticles conjugated with anti-CD19 mAb were shown to detect $CD19^+$ cancer cells. For example, anti-CD19 mAb conjugated hollow gold-silver nanospheres were designed as theranostic agents (Nagy-Simon et al. 2017; Tatar et al. 2019). Besides, anti-CD19 mAb has been successfully used to construct CD19 targeted antibody-drug conjugates (ADCs). Four ADCs targeting $CD19^+$ malignant B cells are in clinical trial now, including SAR3419 (coltuximab ravtansine) (Coiffier et al. 2016; Trneny et al. 2018), SGN-CD19A (denintuzumab mafodotin) (Farhadfar and Litzow, 2016; Jones et al. 2019), ADCT-402 (loncastuximab tesirine) (Krishnan et al. 2015; Zammarchi et al. 2018), and SGN-CD19B (Hicks et al. 2019; Ryan et al. 2017).

As a broad-spectrum anticancer drug, doxorubicin (DOX) is a cytotoxic anthracycline antibiotic isolated from cultures of *Streptomyces peucetius* var. *caesius* (Franco et al. 2018). DOX slows or stops cell growth by blocking topoisomerase 2, and is approved by FDA for the treatment of many types of cancers including

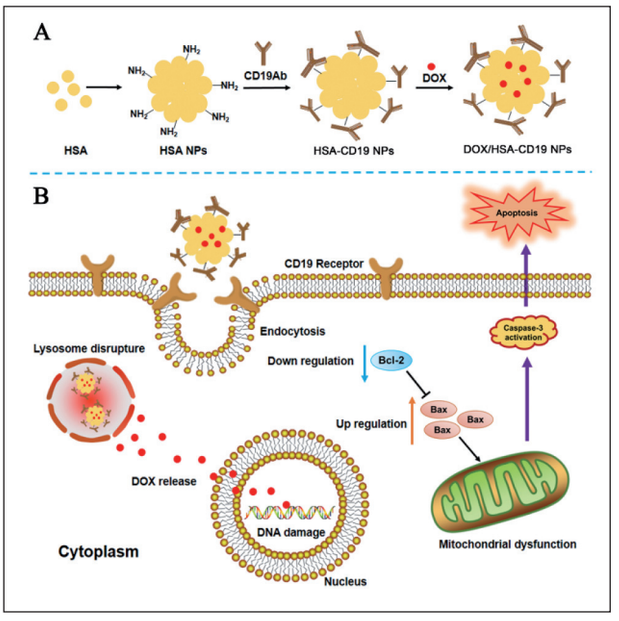

Fig. 1: Schematic illustration of the nanodrug synthesis and the mechanism of nanodrug action. (A) The process of DOX/HSA-CD19 nanodrug synthesis. (B) Targeted delivery of DOX to B-LL cells and resultant apoptosis.

leukemia. However, its clinical application is limited by severe adverse effects such as cardiotoxicity due to the lack of cytotoxic selectivity towards cancer cells over normal cells (Li et al. 2018; Zhang et al. 2015; Zhitnyak et al. 2017) . Therefore, a delivery carrier selectively targeting malignant cells is highly desirable for DOX to reduce the side effects (Zhu et al. 2014). A recent report showed that DOX can be selectively delivered to $CD19^+$ leukemic cells *via* anti-CD19 mAb-conjugated polymeric nanoparticles (Krishnan et al. 2015). Several nanocarriers have been tested, however, human serum albumin (HSA) has not been reported as nanocarrier to conjugate with anti-CD19 mAb for drug delivery purpose. In fact, HSA is an abundant natural material for the fabrication of nanoparticles, and is featured by preferential uptake by tumour cells (Cai et al. 2019; Tzameret et al. 2019; Xu et al. 2018) . In order to develop an effective drug delivery system for DOX to target B-LL cells, we formulated novel anti-CD19 mAb-conjugated HSA nanoparticles (HSA NPs). The HSA NPs were prepared by desolvation, and the following conjugation with anti-CD19 mAb yielded HSA-CD19 nanoparticles (HSA-CD19 NPs). DOX was further encapsulated into the HSA-CD19 NPs to form DOX/HSA-CD19 (Fig. 1A). Through CD19, the DOX/HSA-CD19 efficiently bind to and engulfed by the B-LL cells. Finally, DOX/HSA-CD19 induced apoptosis in B-LL cells (Fig. 1B).

2. Investigations, results and discussion

2.1. Synthesis and characterization of DOX/HSA-CD19 nanodrug

The synthesis of DOX/HSA-CD19 is involving 3 steps: (1) HSA NPs were prepared according to reported desolvation method using glutaraldehyde as a crosslinker. (2) The amino group in HSA NPs was modified by sulfo-SMCC to provide a maleimide crosslinker, while anti-CD19 mAb was treated with 2-iminothiolane hydrochloride to provide an active thiol group for further coupling. Subsequently, HSA NPs and anti-CD19 mAb were coupled by an addition of thiol to maleimide to form HSA-CD19 NPs. (3) The novel nanodrug DOX/HSA-CD19 was obtained by loading DOX into HSA-CD19 NPs. When 2.6 mg of HSA-CD19 NPs was treated with 1 mg of DOX, 20.7% of DOX was encapsulated by HSA-CD19 NPs. The loading content of DOX was 7.35%.
Scanning electron microscope (SEM) and transmission electron microscope (TEM) were used for characterizing the morphology of nanoparticles in nanoscale. The assays showed that synthesized nanoparticles, HSA NPs and DOX/HSA-CD19, displayed spherical shape with average size of 342 nm and 474 nm in diameter, respectively (Fig. 2A-2F), revealing increased size after anti-CD19 mAb conjugation and DOX loading.

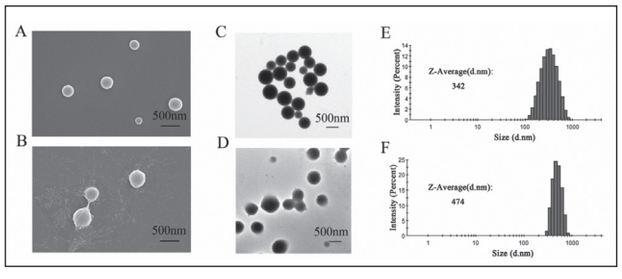

Fig. 2: Characterization of HSA NPs and DOX/HSA-CD19 nanodrug. (A) SEM micrograph of HSA NPs. (B) SEM micrograph of DOX/HSA-CD19. (C) TEM micrograph of HSA NPs. (D) TEM micrograph of DOX/HSA-CD19. (E) The size distribution of HSA NPs. (F) The size distribution of DOX/HSA-CD19.

As shown in Fig. 3, the zeta potentials of nanoparticles were measured. The surface potential of the HSA NPs was -39.2 mV, which was similar to data reported in the literature (Bae et al. 2012). The coupling of anti-CD19 mAb resulted in the increase of the zeta potential of HSA NPs to -18.4 mV. After the loading of DOX, the whole surface potential was further increased to -16.2 mV. The increase of zeta potential suggested that the amino group of DOX is exposed on the nanoparticle surface stably. These results confirmed successful preparation of the nanodrug DOX/HSA-CD19.

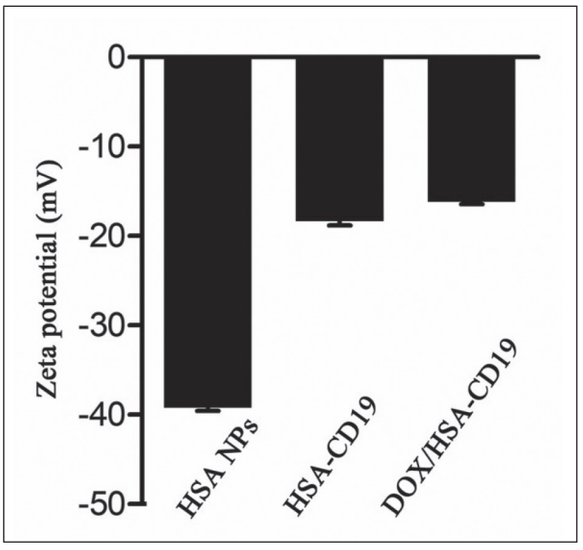

Fig. 3: Zeta potential of nanoparticles measured by DLS. Data were presented as the mean ± SD (n = 3).

2.2. Hemolysis analysis

To evaluate the safety of the DOX/HSA-CD19 in blood, we performed the hemolysis assay. By the ASTM E2524-08 standard, the hemolysis rates of DOX/HSA-CD19 were less than 1% even at 10 μg/mL concentration (Fig. 4). These results suggested that DOX/HSA-CD19 caused negligible damage to the red blood cells, indicating a high safety profile and biocompatibility of DOX/HSA-CD19.

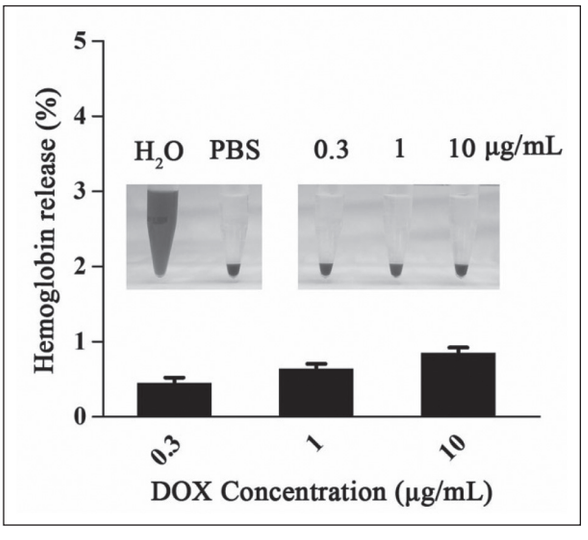

Fig. 4: Hemolysis rate caused by DOX/HSA-CD19 at different concentrations. Data were presented as the mean ± SD (n = 3).

2.3. Specific delivery of DOX/HSA-CD19 to KOPN-8 cells through CD19

To evaluate the specificity of DOX/HSA-CD19 delivery to target cells through CD19, we carried out FACS analysis and confocal microscopy with $CD19^+$ B-LL cell line KOPN-8 and $CD19^-$ monocytic cell line U937. As expected, FACS analysis revealed that

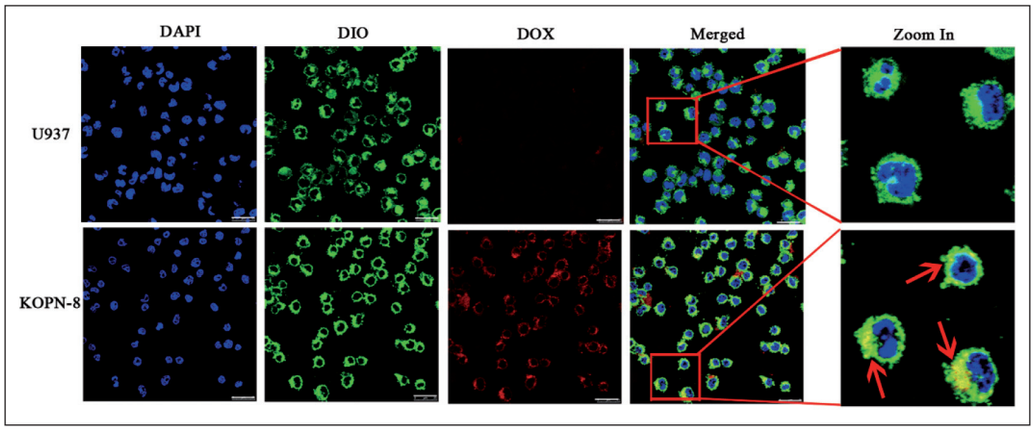

Fig. 5: Targeted delivery of DOX/HSA-CD19 to KOPN-8 cells and U937 cells determined by confocal microscopy. DOX-loaded NPs (DOX concentration, 10 µg/mL) were incubated with KOPN-8 cells and U937 cells for 1 h. Cells were fixed with 4% paraformaldehyde and stained with DIO and DAPI for labelling the cell membranes and nucleus, respectively. Scale bar was 25 µm.

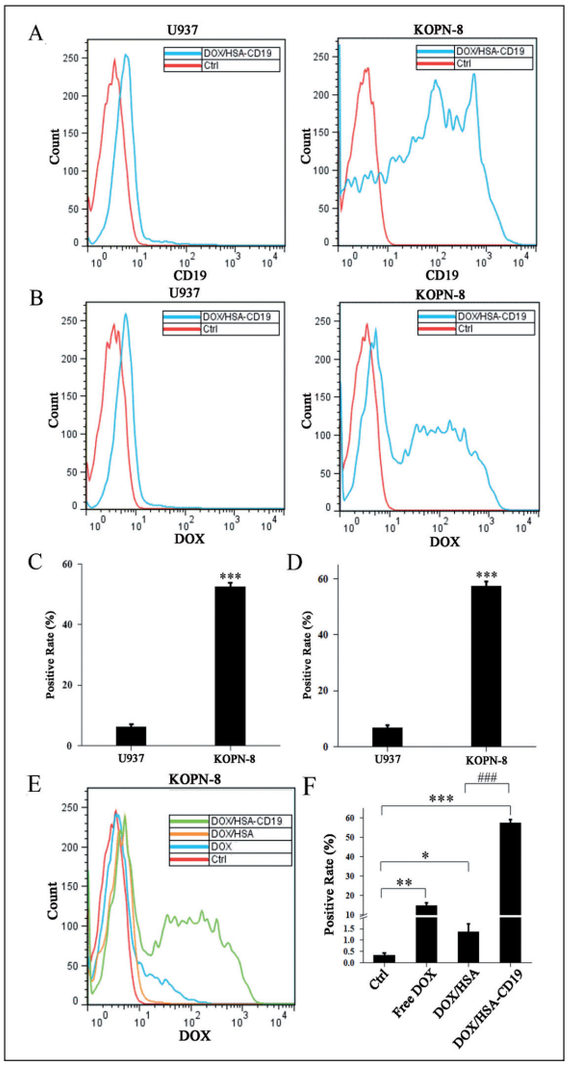

Fig. 6: FACS analysis show cellular uptake rate of nanoparticles. (A) Uptake rate of DOX/HSA-CD19 nanodrug by U937 cells (left) and KOPN-8 cells (right) after exposure to DOX/HSA-CD19 (DOX concentration, 10 µg/mL) for 1 h. DOX/HSA-CD19 nanodrug was identified by anti-CD19 mAb and FITC-fluorescent secondary antibody in U937 cells (left) and KOPN-8 cells (right). (B) Auto-fluorescence of DOX (red) represents DOX/HSA-CD19. (C) Quantitative analysis of (A). (D) Quantitative analysis of (B). (E) Uptake rate of free DOX, DOX/HSA and DOX/HSA-CD19 in KOPN-8 cells. DOX concentration, 10 µg/mL. The untreated cells were used as a control. (F) Quantitative analysis of (E). Data were presented as mean ± SD (n = 3). *p < 0.05; **p < 0.01; ***p<0.001; ###p < 0.001.

99.9% of KOPN-8 cells express CD19, compared to 1.92% of U937 cells.

DOX is naturally autofluorescent and this characteristic can be used to demonstrate and delineate drug delivery by the aid of fluorescence microscopic study. As Fig. 5 shows, confocal microscopy showed that DOX (red signal) was clearly detectable on the membrane of about 65% of KOPN-8 cells, suggesting about 2/3 of KOPN-8 cells have opportunity to uptake DOX. By contrast, less than 7% of U937 cells were positive for DOX. These observations demonstrated that DOX/HSA-CD19 was selectively delivered to KOPN-8 cells with high expression of CD19. The specific delivery of DOX by HSA-CD19 NPs not only facilitates the subsequent cell uptake, but also is beneficial for reducing toxicity to normal cells.

2.4. DOX/HSA-CD19 was efficiently uptaken by KOPN-8 cells

To further evaluate the efficiency of DOX/HSA-CD19 delivery, cellular uptake ability assay was carried out with KOPN-8 and U937 cells. KOPN-8 cells and U937 cells were incubated with DOX/HSA-CD19 for 1h, followed by FITC-labelled secondary antibody. The uptake efficiency was evaluated by FACS. As shown in Fig. 6A and 6C, 52.26% of KOPN-8 cells and only 6.08% of U937 cells uptake DOX/HSA-CD19 when sorted with anti-CD19 antibody. This is an unsurprising result as it showed high correspondence to the data obtained in the delivery assays. The cellular uptake efficiency was further confirmed with auto-fluorescence emitted by DOX. As revealed in Fig. 6B and 6D, 57.32% of KOPN-8 cells but only 6.76% of U937 cells uptake DOX, which was consistent with the result from CD19 sorting. In control experiments, we further found that KOPN-8 cells uptake only 1% of DOX/HSA, and 15% of free DOX, respectively (Fig. 6F). Taken together, these data revealed that anti-CD19 mAb renders significantly increased uptake efficiency and specificity, and the HSA-CD19 NPs are effective carriers to target $CD19^+$ B-LL cells.

2.5. DOX/HSA-CD19 inhibited KOPN-8 cell proliferation

The cytotoxicity of DOX/HSA-CD19 against KOPN-8 target cells was determined by the CCK-8 assay kit. As shown in Fig. 7, DOX/HSA-CD19 strongly inhibited the proliferation of KOPN-8 cells in a dose-dependent manner with an IC_{50} value of 4.1 µg/mL. In the contrary, no significant cytotoxicity of DOX/HSA-CD19 on U937 control cells was found even at 10 µg/mL of DOX concentration. These results indicated a selective therapeutic action of DOX/HSA-CD19 nanodrug on $CD19^+$ B-LL cells, and a good safety profile to $CD19^-$ cells (Fig. 7).

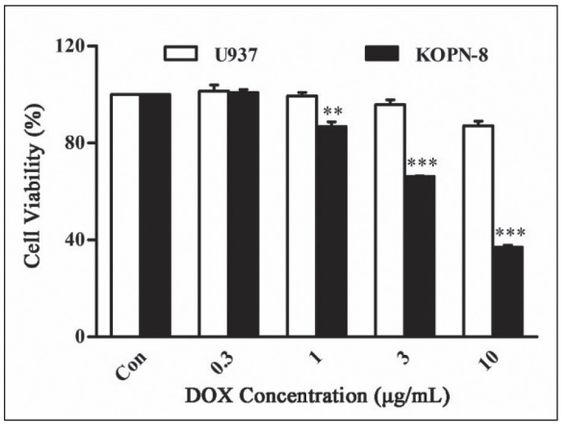

Fig. 7: Cytotoxicity of the nanodrug in KOPN-8 and U937 cells determined by the CCK-8 assay kit. Cell viability of KOPN-8 cells and U937 cells after exposure to DOX/HSA-CD19 for 24 h at a dose range of 0-10 μg/mL was shown. IC_{50}= 4.104 μg/mL. **p <0.01, ***p <0.001. Data were presented as the mean ± SD (n= 3).

2.6. DOX/HSA-CD19 activated the apoptosis pathway in KOPN-8 cells

DOX is known to induce apoptosis and DNA damage (Tacar et al. 2013). We further conducted western blotting assays to evaluate the apoptotic effect of DOX/HSA-CD19 on KOPN-8 cells. We found that antiapoptotic protein Bcl-2 was significantly downregulated, and proapoptotic proteins, Bax and caspase-3, were strikingly upregulated in KOPN-8 cells treated with DOX/HSA-CD19 (Fig. 8A, 8B). This result confirmed that similarly to DOX, DOX/HSA-CD19 nanodrug activates the apoptosis pathway to destroy KOPN-8 cells.

In conclusion, HSA-CD19 NPs showed promising ability for loading, selectively delivering and facilitating the cell uptake of anticancer agents DOX towards $CD19^+$ cells such as KOPN-8. DOX/HSA-CD19 exhibited a good safety profile and biocompatibility as it did not cause damage to red blood cells and normal $CD19^-$ cells as well. DOX/HSA-CD19 exhibited effective cytotoxicity against $CD19^+$ cells through the induction of apoptosis in a similar manner with DOX. Taken together, these features of DOX/HSA-CD19 make it a promising nanomedicine for the treatment of B-LL. The *in vivo* biological evaluation of DOX/HSA-CD19 is ongoing.

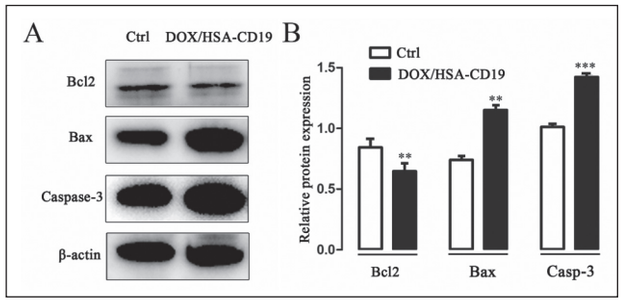

Fig. 8: Western blotting assay shows the activation of apoptosis pathway by the nanodrug. (A) The expression level of apoptosis related proteins. Bcl2 was reduced but Bax and caspase-3 were increased in KOPN-8 cells treated with DOX/HSA-CD19 (DOX concentration, 10 μg/mL) for 24h. (B) Quantitative analysis of (A). **p <0.01, ***p <0.001. Data were presented as mean ± SD (n = 3).

3. Experimental

3.1. Materials

Human serum albumin (HSA, 99%, 66.5 kDa) was obtained from Sigma Aldrich (St. Louis, MO). Anti-CD19 mAb was designed and synthesized by Healsun Biopharm (Hangzhou, China). Doxorubicin•HCl was purchased from Cool Chemistry (Beijing, China). Glutaraldehyde (50%) and ethanol were purchased from Aladdin (Shanghai, China). 2-Iminothiolane hydrochloride and sulfosuccinimidyl 4-(N-maleimidomethyl) cyclohexane-1-carboxylate (sulfo-SMCC) were obtained from Macklin (Shanghai, China). Cell Counting Kit-8 (CCK-8) was purchased from Sangon Biotech (Shanghai, China). Anti-Human CD19-PE and Anti-Mouse CD16/CD32 were purchased from eBioscience (Boston, USA). FITC conjugated Goat anti-rabbit IgG (H+L), Bax Mouse Monoclonal antibody, Bcl2 Mouse Monoclonal antibody, Caspase-3 Mouse Monoclonal antibody were bought from Proteintech Group, Inc (Chicago, USA). Penicillin and streptomycin were purchased from Sangon Biotech (Shanghai, China). RPMI 1640 culture medium was obtained from HyClone (Logan, USA). Fetal bovine serum (FBS) was purchased from Gibco (Boston, USA). 3, 3′-dioctadecyloxacarbocyanine perchlorate (DIO) and 4′, 6-diamidino-2-phenylindole (DAPI) were purchased from Beyotime Biotechnology (Shanghai, China).

3.2. Cell culture

KOPN-8 cell line and U937 cell line were obtained from the Cell Bank of the Chinese Academy of Sciences (Shanghai, China). Cells were cultured in RPMI 1640 containing 10% fetal bovine serum (FBS), 100 U/mL penicillin and 100 U/mL streptomycin at 37 °C in a humidified atmosphere containing 5% CO_2.

3.3. Preparation of HSA NPs

HSA NPs were prepared by desolvation technique according to reported procedures (Jahanban-Esfahlan et al. 2016; Wilson et al. 2014) . Briefly, HSA (20 mg) was dissolved in deionized water (1 mL), and sonicated for 5 min. To the HSA solution, was added absolute ethanol (8 mL) at a rate of 1 mL/min with a stirring speed of 1000 rpm. Then, 8% glutaraldehyde (23.6 μL) was added, and the mixture was allowed to stir at room temperature for 12 h. The product was collected by centrifugation at 8000 rpm for 10 min. The precipitate was washed three times with deionized water to remove any remaining HSA and glutaraldehyde. The obtained HSA NPs were resuspended in deionized water and stored at 4 °C.

3.4. Preparation of HSA-CD19 NPs

HSA-CD19 NPs were prepared using a modified literature procedure (Choi et al. 2015; Hoppmann et al. 2011). To a suspension of HSA NPs (3 mg) in deionized water, sulfo-SMCC (1 mg) was added. The resulting mixture was stirred for 3 h at room temperature. The activated SMCC-HSA NPs were obtained by centrifugation at 8000 rpm for 10 min to remove unbound sulfo-SMCC. Besides, 2-iminothiolane hydrochloride (5.5 μg) was added to anti-CD19 mAb (1 mg in deionized water), and the mixture was stirred at room temperature for 1 h to provide HS-CD19. Then, the HS-CD19 was added dropwise to the activated SMCC-HSA NPs. The mixture was stirred for another 3 h at room temperature. The pellets were washed with deionized water three times to afford purified HSA-CD19 NPs.

3.5. DOX loading in HSA NPs and HSA-CD19

DOX•HCl (1 mg/mL in deionized water) was added dropwise into a suspension of HSA NPs and HSA-CD19 NPs in deionized water, respectively. The resulting suspension was stirred at room temperature for 6 h. The pellets were washed with deionized water three times to remove unloaded DOX•HCl. Eventually, DOX/HSA and DOX/HSA-CD19 were obtained, respectively (Thao le et al. 2016; Wang et al. 2014).

The drug loading content (LC) was calculated by the formula below:

$$LC\ (\%) = W_D/(W_N + W_D) \times 100\% \quad (1)$$

where W_D is the amount of DOX in the particles, W_N is the amount of the nanoparticles before drug loading.

3.6. Characterization of prepared nanoparticles

The morphology of prepared nanoparticles was observed under SEM (Nova Nano SEM 450, FEI, USA) and TEM (Tecnai G2F30 STWIN, FEI, USA). The size and zeta potential of nanoparticles were measured by Malvern Zetasizer Nano ZS (Nano ZS90, Malvern, UK). Nanoparticles were diluted 1:500 with deionized water and the size was measured at 25 °C.

3.7. Hemolysis assay

The red blood cells of rabbit were used for hemolysis assay. Blood cells were prepared from the whole blood obtained from rabbit heart by centrifugation. The red blood cells were washed three times with PBS (pH7.4) and resuspended in PBS. The DOX/HSA-CD19 were diluted to different concentrations of 0.3, 1, 10 μg/mL in 1 mL with PBS. To each well containing red blood cells (50 μL), was added above nanodrugs, deionized water and PBS, respectively. Deionized water and PBS were used as positive control and negative control, respectively. After incubation in the shaker at 37 °C for 2 h, the absorbance was measured at 540 nm by the microplate reader (Synergy H1, Biotek, USA). The hemolysis rate was calculated by the formula below:

$$\text{Hemolysis}\ (\%) = (Abs_{drug} - Abs_{negative})/(Abs_{positive} - Abs_{negative}) \times 100\% \quad (2)$$

3.8. The expression of CD19 in U937 and KOPN-8 cells

The expression of CD19 was detected by Flow cytometry (BD FACSCalibur, USA). Briefly, U937 and KOPN-8 cells were blocked by anti-mouse CD16/CD32 for 15 min, then incubated on ice with anti-CD19-PE for 40 min. Unbound anti-CD19 mAb was removed by centrifugation.

3.9. Targeted delivery of DOX/HSA-CD19

KOPN-8 and U937 cells were seeded into a 24-well plate (1.5×10^5 cells/well), and the DOX/HSA-CD19 (DOX concentration, 10 μg/mL) were added and co-incubated for 1

h at 37 °C. Then, the cells were collected by centrifugation and the followed removal of the supernatant. The collected cells were fixed on a glass slide. Paraformaldehyde (4%) was added to fix the cells for 15 min. After washing with PBS, 400 μL of cell membrane dye DIO and nucleus dye DAPI were sequentially added (Gothwal et al. 2018; Wathiong et al. 2019). The cells were observed under a confocal laser scanning microscope (DMI6000CS, Leica, Germany).

3.10. Cellular uptake assay

KOPN-8 and U937 cells (1×10^6 cells/well) were seeded into a 6-well plate. The free DOX, DOX/HSA and DOX/HSA-CD19 (DOX concentration, 10 μg/mL) were added to cells and incubated for 1 h, respectively. The red fluorescence of DOX and the FITC-fluorescent secondary antibody were used to evaluate the cellular uptake of DOX, DOX/HSA and DOX/HSA-CD19 by FACS (Rades et al. 2019; Soleymani et al. 2019).

3.11. Cytotoxicity in vitro

To evaluate the cytotoxicity of nanoparticles, KOPN-8 and U937 cells were seeded into 96-well plate at 5000 cells/well with RPMI 1640 (100 μL), respectively. The DOX/HSA-CD19 with DOX at concentrations of 0.3, 1, 3, 10 μg/mL were added to the cells, respectively. After incubation for 24 hours, CCK-8 kit (10 μL) was added to each well and incubated for another 2 hours. Finally, the absorbance at 450 nm was measured by microplate reader (Synergy H1, Biotek, USA).

3.12. Western blotting analysis

The protein expression of caspase-3, apoptosis promoting protein Bax and apoptosis inhibitory protein Bcl2 were determined by western blotting (Deng et al. 2018; Song et al. 2018). KOPN-8 cells were seeded into a 6-well plate (1×10^6 cells/well). DOX/HSA-CD19 with DOX at 10 μg/mL was added and co-incubated for 24 h. The collected cells were lysed on ice for 30 min, followed by centrifugation at 13300 rpm for 10 min.

Cell proteins (20 μg) were loaded. Then, the cell lysates were separated by sodium dodecyl sulfate-polyacrylamide gel electrophoresis (SDS-PAGE) and transferred to 0.45 μm PVDF membranes. Skim milk (5%) was used to block for 1 h, and the PVDF membranes were incubated with the corresponding primary antibody (Bax Rabbit polyclonal antibody, 1:1000; Bcl2 Rabbit polyclonal antibody, 1:2000; Caspase-3 Rabbit polyclonal antibody, 1:1000) overnight at 4 °C and followed by secondary antibody (HRP-labeled Goat Anti-Rabbit IgG (H+L), 1:1000) for 1 h at room temperature. The expression level of proteins was determined by chemiluminescence immunoassay using the Imaging System (FluorChem HD2, ProteinSimple, USA).

Acknowledgements: This work was supported by the National Natural Science Foundation of Liaoning Province (No. 20170540184).

Conflicts of interest: There are no conflicts of interest to declare.

References

Akiyama M, Yamada O, Agawa M, Yuza Y, Yanagisawa T, Eto Y, Yamada H (2008) Effects of prednisolone on specifically expressed genes in pediatric acute B–lymphoblastic leukemia. J Pediatr Hematol Oncol 30: 313–316.

Bae S, Ma K, Kim TH, Lee ES, Oh KT, Park ES, Lee KC, Youn YS (2012) Doxorubicin-loaded human serum albumin nanoparticles surface–modified with TNF-related apoptosis-inducing ligand and transferrin for targeting multiple tumor types. Biomaterials 33: 1536–1546.

Bray F, Ferlay J, Soerjomataram I, Siegel RL, Torre LA, Jemal A (2018) Global cancer statistics 2018: GLOBOCAN estimates of incidence and mortality worldwide for 36 cancers in 185 countries. CA Cancer J Clin 68: 394–424.

Cai G, Wang S, Zhao L, Sun Y, Yang D, Lee RJ, Zhao M, Zhang H, Zhou Y (2019) Thiophene derivatives as anticancer agents and their delivery to tumor cells using albumin nanoparticles. Molecules 24: pii E192.

Choi SH, Byeon HJ, Choi JS, Thao L, Kim I, Lee ES, Shin BS, Lee KC, Youn YS (2015) Inhalable self–assembled albumin nanoparticles for treating drug–resistant lung cancer. J Control Release 197: 199–207.

Coiffier B, Thieblemont C, de Guibert S, Dupuis J, Ribrag V, Bouabdallah R, Morschhauser F, Navarro R, Le Gouill S, Haioun C, Houot R, Casasnovas O, Holte H, Lamy T, Broussais F, Payrard S, Hatteville L, Tilly H (2016) A phase II, single–arm, multicentre study of coltuximab ravtansine (SAR3419) and rituximab in patients with relapsed or refractory diffuse large B–cell lymphoma. Br J Haematol 173: 722–730.

Deng M, Zha J, Jiang Z, Jia X, Shi Y, Li P, Chen XL, Fang Z, Du Z, Xu B (2018) Apatinib exhibits anti-leukemia activity in preclinical models of acute lymphoblastic leukemia. J Transl Med 16: 47.

Farhadfar N, Litzow MR (2016) New monoclonal antibodies for the treatment of acute lymphoblastic leukemia. Leuk Res 49: 13–21.

Franco YL, Vaidya TR, Ait–Oudhia S (2018) Anticancer and cardio–protective effects of liposomal doxorubicin in the treatment of breast cancer. Breast Cancer 10: 131–141.

Ghorashian S, Kramer AM, Onuoha S, Wright G, Bartram J, Richardson R, Albon SJ, Casanovas–Company J, Castro F, Popova B, Villanueva K, Yeung J, Vetharoy W, Guvenel A, Wawrzyniecka PA, Mekkaoui L, Cheung GW, Pinner D, Chu J, Lucchini G, Silva J, Ciocarlie O, Lazareva A, Inglott S, Gilmour KC, Ahsan G, Ferrari M, Manzoor S, Champion K, Brooks T, Lopes A, Hackshaw A, Farzaneh F, Chiesa R, Rao K, Bonney D, Samarasinghe S, Goulden N, Vora A, Veys P, Hough R, Wynn R, Pule MA, Amrolia PJ (2019) Enhanced CAR T cell expansion and prolonged persistence in pediatric patients with ALL treated with a low–affinity CD19 CAR. Nat Med 25: 1408–1414.

Giavridis T, van der Stegen SJC, Eyquem J, Hamieh M, Piersigilli A, Sadelain M (2018) CAR T cell-induced cytokine release syndrome is mediated by macrophages and abated by IL-1 blockade. Nat Med 24: 731–738.

Gothwal A, Khan I, Kumar P, Raza K, Kaul A, Mishra AK, Gupta U (2018) Bendamustine-PAMAM conjugates for improved apoptosis, efficacy, and in vivo pharmacokinetics: a sustainable delivery tactic. Mol Pharm 15: 2084–2097.

Hicks SW, Tarantelli C, Wilhem A, Gaudio E, Li M, Arribas AJ, Spriano F, Bordone R, Cascione L, Lai KC, Qiu Q, Taborelli M, Rossi D, Stussi G, Zucca E, Stathis A, Sloss CM, Bertoni F (2019) The novel CD19–targeting antibody–drug conjugate huB4–DGN462 shows improved anti–tumor activity compared to SAR3419 in CD19–positive lymphoma and leukemia models. Haematologica 104: 1633–1639.

Hoppmann S, Miao Z, Liu S, Liu H, Ren G, Bao A, Cheng Z (2011) Radiolabeled affibody-albumin bioconjugates for HER2–positive cancer targeting. Bioconjug Chem 22: 413–421.

Jahanban–Esfahlan A, Dastmalchi S, Davaran S (2016) A simple improved desolvation method for the rapid preparation of albumin nanoparticles. Int J Biol Macromol 91: 703–709.

Jones L, McCalmont H, Evans K, Mayoh C, Kurmasheva RT, Billups CA, Houghton PJ, Smith MA, Lock RB (2019) Preclinical activity of the antibody–drug conjugate denintuzumab mafodotin (SGN-CD19A) against pediatric acute lymphoblastic leukemia xenografts. Pediatr Blood Cancer 66: e27765.

Krishnan V, Xu X, Kelly D, Snook A, Waldman SA, Mason RW, Jia X, Rajasekaran AK (2015) CD19-targeted nanodelivery of doxorubicin enhances therapeutic efficacy in B-cell acute lymphoblastic leukemia. Mol Pharm 12: 2101–2111.

Li M, Sala V, De Santis MC, Cimino J, Cappello P, Pianca N, Di Bona A, Margaria JP, Martini M, Lazzarini E, Pirozzi F, Rossi L, Franco I, Bornbaum J, Heger J, Rohrbach S, Perino A, Tocchetti CG, Lima BHF, Teixeira MM, Porporato PE, Schulz R, Angelini A, Sandri M, Ameri P, Sciarretta S, Lima–Junior RCP, Mongillo M, Zaglia T, Morello F, Novelli F, Hirsch E, Ghigo A (2018) Phosphoinositide 3-kinase gamma inhibition protects from anthracycline cardiotoxicity and reduces tumor growth. Circulation 138: 696–711.

Nagy–Simon T, Tatar AS, Craciun AM, Vulpoi A, Jurj MA, Florea A, Tomuleasa C, Berindan–Neagoe I, Astilean S, Boca S (2017) Antibody conjugated, Raman tagged hollow gold-silver nanospheres for specific targeting and multimodal dark-field/SERS/two photon-FLIM imaging of CD19(+) B lymphoblasts. ACS Appl Mater Interfaces 9: 21155–21168.

Rades N, Achazi K, Qiu M, Deng C, Haag R, Zhong Z, Licha K (2019) Reductively cleavable polymer-drug conjugates based on dendritic polyglycerol sulfate and monomethyl auristatin E as anticancer drugs. J Control Release 300: 13–21.

Ryan MC, Palanca–Wessels MC, Schimpf B, Gordon KA, Kostner H, Meyer B, Yu C, Van Epps HA, Benjamin D (2017) Therapeutic potential of SGN-CD19B, a PBD–based anti–CD19 drug conjugate, for treatment of B–cell malignancies. Blood 130: 2018–2026.

Schuster SJ, Bishop MR, Tam CS, Waller EK, Borchmann P, McGuirk JP, Jäger U, Jaglowski S, Andreadis C, Westin JR, Fleury I, Bachanova V, Foley SR, Ho PJ, Mielke S, Magenau JM, Holte H, Pantano S, Pacaud LB, Awasthi R, Chu J, Anak Ö, Salles G, Maziarz RT (2019) Tisagenlecleucel in adult relapsed or refractory diffuse large B-cell lymphoma. N Engl J Med 380: 45–56.

Soleymani J, Hasanzadeh M, Somi MH, Shadjou N, Jouyban A (2019) Highly sensitive and specific cytosensing of HT 29 colorectal cancer cells using folic acid functionalized-KCC-1 nanoparticles. Biosens Bioelectron 132: 122–131.

Song B, Chen Y, Liu Y, Wan C, Zhang L, Zhang W (2018) NPAS2 regulates proliferation of acute myeloid leukemia cells via CDC25A–mediated cell cycle progression and apoptosis. J Cell Biochem: doi: 10.1002/jcb.28160.

Tacar O, Sriamornsak P, Dass CR (2013) Doxorubicin: an update on anticancer molecular action, toxicity and novel drug delivery systems. J Pharm Pharmacol 65: 157–170.

Tatar AS, Jurj A, Tomuleasa C, Florea A, Berindan-Neagoe I, Cialla-May D, Popp J, Astilean S, Boca S (2019) CD19–targeted, Raman tagged gold nanourchins as theranostic agents against acute lymphoblastic leukemia. Colloids Surf B Biointerfaces 184: 110478.

Thao le Q, Byeon HJ, Lee C, Lee S, Lee ES, Choi YW, Choi HG, Park ES, Lee KC, Youn YS (2016) Doxorubicin-bound albumin nanoparticles containing a TRAIL protein for targeted treatment of colon cancer. Pharm Res 33: 615–626.

Trneny M, Verhoef G, Dyer MJ, Ben Yehuda D, Patti C, Canales M, Lopez A, Awan FT, Montgomery PG, Janikova A, Barbui AM, Sulek K, Terol MJ, Radford J, Guidetti A, Di Nicola M, Siraudin L, Hatteville L, Schwab S, Oprea C, Gianni AM (2018) A phase II multicenter study of the anti-CD19 antibody drug conjugate coltuximab ravtansine (SAR3419) in patients with relapsed or refractory diffuse large B–cell lymphoma previously treated with rituximab-based immunotherapy. Haematologica 103: 1351–1358.

Tzameret A, Ketter-Katz H, Edelshtain V, Sher I, Corem–Salkmon E, Levy I, Last D, Guez D, Mardor Y, Margel S, Rotenstrich Y (2019) In vivo MRI assessment of bioactive magnetic iron oxide/human serum albumin nanoparticle delivery into the posterior segment of the eye in a rat model of retinal degeneration. J Nanobiotechnology 17: 3.

Wang D, Xu Z, Yu H, Chen X, Feng B, Cui Z, Lin B, Yin Q, Zhang Z, Chen C, Wang J, Zhang W, Li Y (2014) Treatment of metastatic breast cancer by combination of chemotherapy and photothermal ablation using doxorubicin-loaded DNA wrapped gold nanorods. Biomaterials 35: 8374–8384.

Wang K, Wei G, Liu D (2012) CD19: a biomarker for B cell development, lymphoma diagnosis and therapy. Exp Hematol Oncol 1: 36.

Wathiong B, Deville S, Jacobs A, Smisdom N, Gervois P, Lambrichts I, Ameloot M, Hooyberghs J, Nelissen I (2019) Role of nanoparticle size and sialic acids in the distinct time–evolution profiles of nanoparticle uptake in hematopoietic progenitor cells and monocytes. J Nanobiotechnology 17: 62.

Wei G, Wang J, Huang H, Zhao Y (2017) Novel immunotherapies for adult patients with B-lineage acute lymphoblastic leukemia. J Hematol Oncol 10: 150.

Wilson B, Lavanya Y, Priyadarshini SR, Ramasamy M, Jenita JL (2014) Albumin nanoparticles for the delivery of gabapentin: preparation, characterization and pharmacodynamic studies. Int J Pharm 473: 73–79.

Xu H, Hua Y, Zhong J, Li X, Xu W, Cai Y, Mao Y, Lu X (2018) Resveratrol delivery by albumin nanoparticles improved neurological function and neuronal damage in transient middle cerebral artery occlusion rats. Front Pharmacol 9: 1403.

Yang Y, Zhao W, Tan W, Lai Z, Fang D, Jiang L, Zuo C, Yang N, Lai Y (2019) An efficient cell-targeting drug delivery system based on aptamer-modified mesoporous silica nanoparticles. Nanoscale Res Lett 14: 390.

Zammarchi F, Corbett S, Adams L, Tyrer PC, Kiakos K, Janghra N, Marafioti T, Britten CE, Havenith CEG, Chivers S, D'Hooge F, Williams DG, Tiberghien A, Howard PW, Hartley JA, van Berkel PH (2018) ADCT-402, a PBD dimer-containing antibody drug conjugate targeting CD19–expressing malignancies. Blood 131: 1094–1105.

Zhang Z, Yu X, Wang Z, Wu P, Huang J (2015) Anthracyclines potentiate anti–tumor immunity: A new opportunity for chemoimmunotherapy. Cancer Letters 369: 331–335.

Zhitnyak IY, Bychkov IN, Sukhorukova IV, Kovalskii AM, Firestein KL, Golberg D, Gloushankova NA, Shtansky DV (2017) Effect of BN nanoparticles loaded with doxorubicin on tumor cells with multiple drug resistance. ACS Appl Mater Interfaces 9: 32498–32508.

Zhu Q, Jia L, Gao Z, Wang C, Jiang H, Zhang J, Dong L (2014) A tumor environment responsive doxorubicin–loaded nanoparticle for targeted cancer therapy. Mol Pharm 11: 3269–3278.